

## Online Data Supplements

1  
2  
3  
4  
5  
6  
7  
8  
9  
10  
11  
12  
13

Bioactive Metabolites Derangements Differentiating Idiopathic and Scleroderma  
Associated Pulmonary Arterial Hypertension

Mona Alotaibi MD<sup>1</sup>, Junzhe Shao<sup>2</sup>, Michael W. Pauciulo MBA<sup>3,4</sup>, William C. Nichols  
PhD<sup>3,4</sup>, Anna R. Hemnes MD<sup>5</sup>, Atul Malhotra MD<sup>1</sup>, Nick H. Kim MD<sup>1</sup>, Jason X.-J. Yuan  
MD PhD<sup>1</sup>, Timothy Fernandes MD<sup>1</sup>, Kim M. Kerr MD<sup>1</sup>, Laith Alshwabkeh MD<sup>6</sup>, Ankit A.  
Desai MD<sup>8</sup>, Jeramie D. Watrous PhD<sup>7</sup>, Susan Cheng MD MPH MMsc<sup>9</sup>, Tao Long PhD<sup>7</sup>,  
Stephen Y. Chan MD PhD<sup>10</sup>, Mohit Jain MD PhD<sup>7</sup>

14 **eMethods:**

15 *Sample preparation*

16 Plasma samples were thawed at 4C overnight; 20  $\mu$ L of plasma was transferred into a  
17 96-well extraction plate. Proteins were precipitated with the addition of 80  $\mu$ L of ice-cold  
18 extraction solvent (consisting of ethanol for reverse phase method and a mixture of  
19 45:45:10 methanol:ACN:water for the HILIC method), as described.<sup>1-3</sup> Plates were  
20 sealed, vortexed and centrifuged to precipitate proteins with the supernatant containing  
21 extract metabolites pipetted into a clean microtiter plate for LC-MS analysis. For the  
22 reverse phase methods, samples were passed across a reverse phase SPE column  
23 (Phenomenex 8B-S199-UB), and lipid species eluted using 1ml methanol, as  
24 described<sup>1,3</sup>, before being transferred into a clean microtiter plate for LC-MS analysis.

25  
26 *Metabolite Assay*

27  
28 Bioactive metabolites analysis was performed on plasma samples using state of the art  
29 LC-MS, using a Vanquish UPLC coupled to high resolution, QExactive orbitrap mass  
30 spectrometer (Thermo). Multiple complementary LC methods were performed, each  
31 optimized to capture a chemical subset of bioactive metabolites, including polar  
32 molecules like sugars and organic acids (using Zic-pHILIC 2.1x150mm 5um column) and  
33 small polar, bioactive lipids (using a Phenomenex Kinetex C18 column). All generated  
34 spectral data underwent daily Qc/Qa analysis, as described in the section below. Data  
35 was extracted using image processing and machine learning based spectral optimization.  
36 Each sample MS data file was initially represented as an image using mass to charge  
37 and retention time coordinates. A watershed algorithm was applied to image files using  
38 peak apex density as a guide to define regions containing putative spectral peaks. An

39 optimized neural network was subsequently applied to all putative spectra peaks to isolate  
40 true spectral peaks from 'false' background signals. Following data extraction, spectral  
41 peaks were cross aligned among datasets using landmark based algorithms to allow for  
42 comparison of signals among cohorts. Data was subsequently normalized to account for  
43 plate-to-plate variation using a simple batch median normalization metric with correction  
44 for median absolute deviation. Following normalization, metabolite peaks were further  
45 compressed for multiple adducts and in source fragments. Normalized, aligned, filtered  
46 datasets were subsequently used for statistical analyses, as described below. Metabolites  
47 were annotated by using an in-house library of commercially available standards or  
48 MS/MS fragmentation patterns.

49

#### 50 *QC/QA of Spectral data.*

51 Qc/Qa of data has been standardized using a panel of deuterated internal standards as  
52 well as interval pooled plasma samples to monitor fluctuations in extraction efficiency,  
53 instrument sensitivity, matrix artifact and mass accuracy. Any samples not meeting Qc/Qa  
54 thresholds underwent reinjection. The assay was highly reproducible over several days  
55 and independent measures with median coefficient of variance (CV) across analytes at  
56 low standard concentrations of 0.15 ng.

57

58 Table 1e. Supplements: Medications

	Discovery cohort			1 <sup>st</sup> Validation cohort		
	IPAH	SSc-PAH	<i>P</i>	IPAH	SSc-PAH	<i>P</i>
N	864	310		213	91	
Warfarin (%)	326 (37.7)	41 (13.2)	<0.001	93 (43.7)	18 (19.8)	<0.001
Heparin (%)	3 (0.3)	2 (0.6)	0.855	213 (100.0)	91 (100.0)	NA
Corticosteroid (%)	57 (6.6)	70 (22.6)	<0.001	34 (16.0)	30 (33.0)	0.001
Aspirin (%)	180 (20.8)	105 (33.9)	<0.001	43 (20.2)	32 (35.2)	0.009
NSAID (%)	53 (6.1)	30 (9.7)	0.05	23 (10.8)	10 (11.0)	1
Immunosuppressive medications (%)	15 (1.7)	70 (22.6)	<0.001	5 (2.3)	20 (22.0)	<0.001
Synthetic Thyroid (%)	158 (18.3)	95 (30.6)	<0.001	49 (23.0)	40 (44.0)	<0.001

59

60

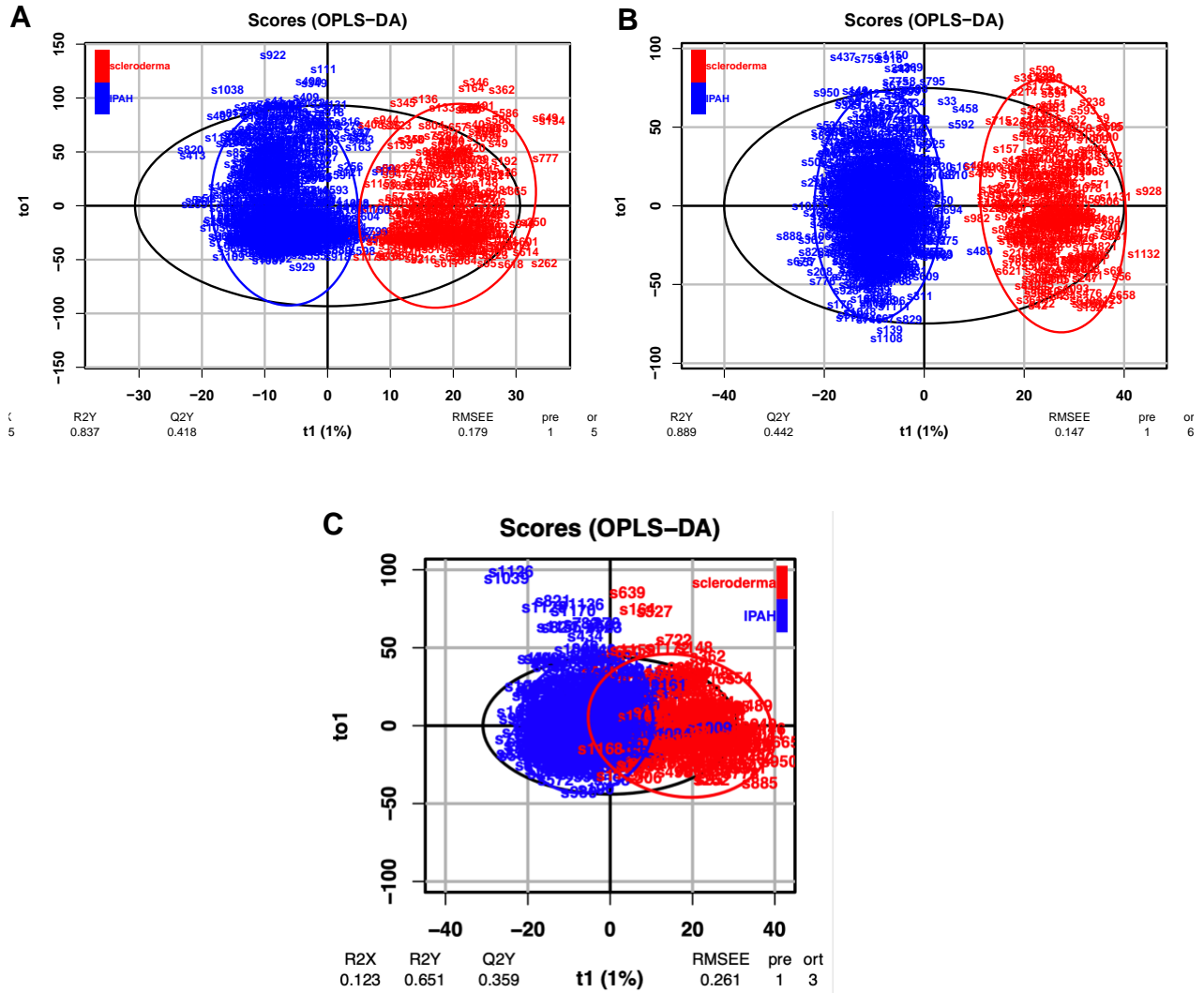
61

62

63 **Figure 1e. Orthogonal partial least squares-discriminant analysis (OPLS-DA) plots**  
 64 **analysis of bioactive lipids and HILIC metabolites.**

- 65 A. Scores plot of the OPLS-DA model for bioactive lipids metabolites.  
 66 B. Scores plot of the OPLS-DA model for the HILIC positive metabolites.  
 67 C. Scores plot of the OPLS-DA model for the HILIC negative metabolites.

68  
 69



70

71 eReferences:

72

73 1. Watrous JD, Niiranen TJ, Lagerborg KA, Henglin M, Xu YJ, Rong J, Sharma S,

74 Vasan RS, Larson MG, Armando A et al. 2019. Directed non-targeted mass

75 spectrometry and chemical networking for discovery of eicosanoids and related

76 oxylipins. *Cell Chem Biol.* 26(3):433-442.e434.

77 2. Lagerborg KA, Watrous JD, Cheng S, Jain M. 2019. High-throughput measure of

78 bioactive lipids using non-targeted mass spectrometry. *Methods Mol Biol.* 1862:17-35.

79 3. Kantz ED, Tiwari S, Watrous JD, Cheng S, Jain M. 2019. Deep neural networks for

80 classification of lc-ms spectral peaks. *Anal Chem.* 91(19):12407-12413.

81

82